Experimental Calibration of a Viscoplastic-fracturing Computational Model

A. Scarpas[1], J. Blaauwendraad[1], R. Al-Khoury[2] and C. van Gurp[2]
[1]*Faculty of Civil Engineering, TU-Delft, Stevinweg 1, 2628 CN Delft, The Netherlands. Email: scarpas@ct.tudelft.nl*
[2]*KOAD-WMD, Schumanpark 43, 7336 AS, Apeldoorn, The Netherlands*

Abstract

An extensive experimental and analytical investigation is currently being carried out on the mechanisms leading to the initiation and propagation of damage in viscoplastic materials. One of the major goals of the investigation is the development and the finite elements implementation of a generalised triaxial, strain rate sensitive, history and temperature dependent constitutive model. Explicit procedures have been formulated for the experimental determination of the model parameters. As a minimum, only uniaxial test results are needed for determination of the basic parameters. The model has been implemented in the finite element code CAPA-3D. Results of the utilization of CAPA-3D for the investigation of the dynamic non-linear response of a road pavement are reviewed in the last part of this contribution.

1 Introduction

Currently, the finite element method is being utilized in several engineering fields for the purpose of understanding the role and the contribution of the engineering properties (e.g. material stiffness, material strength, fracture energy) of the constituent materials of a structure in the overall response (e.g. deflections, load carrying capacity etc.). A pre-requisite for utilization of the method is the availability of material constitutive models capable of describing the triaxial behaviour in the linear and the non-linear ranges.

Because of the importance of non-linearity on material response, an extensive project of investigation has been initiated by the authors whose goal is the development of a constitutive model for the characterization of the material response of viscoplastic materials, under realistic -triaxial- conditions. An elasto-viscoplastic-fracturing hierarchical formulation has been adopted.

For model calibration purposes, an asphaltic material was chosen to be tested experimentally because it exhibits a wide range of response ranging from elastic to viscoplastic to fracturing and it also experiences rate and temperature dependence. Thus it reflects many of the response characteristics of other engineering materials. On the basis of these tests, the main components of the model and their interaction

were identified. Procedures were developed for the experimental determination of all necessary material parameters.

2 Concepts of viscous material response simulation

The Perzyna (1) formulation of viscoplasticity has been chosen as the most suitable constitutive framework for modelling the time dependent response, Fig. 1, and has been implemented into the finite element method system CAPA-3D (2). In this the viscoplastic strain rate is computed by means of an a-priori postulated flow rule as :

$$\dot{\varepsilon}_{vp} = \Gamma \cdot <\Phi> \cdot \frac{\partial g}{\partial \sigma} \qquad (1)$$

in which Γ is an experimentally determined parameter termed the fluidity parameter, Φ is the viscoplastic flow function, and $\partial g/\partial \sigma$ some measure of the direction of viscoplastic straining.

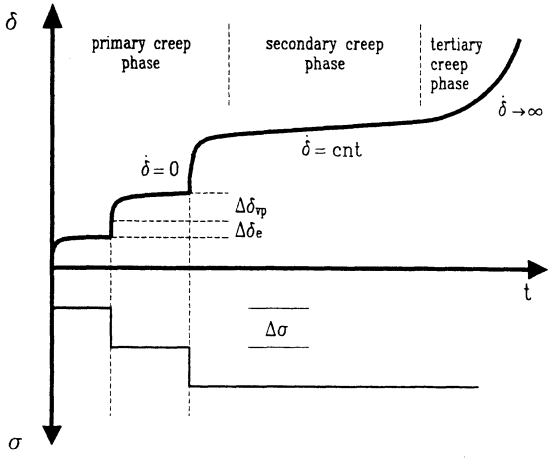

Fig. 1 Schematic of an incremental creep test

2.1 Primary and secondary creep phase simulation

Simulation of the primary and secondary phases of creep flow by means of the proposed model and a methodology for the experimental determination of those model parameters pertaining to these two stages of material response has been presented in another publication, Scarpas et al. (3). In this contribution, discussion will focus on those aspects of the model related to the tertiary phase of response.

3 Material strength degradation due to viscous flow

If in an incremental creep test, Fig. 1, the time Δt between successive stress increments is reduced, the full extent of the viscous flow is not allowed to occur and a stiffening effect, manifesting itself as a strength increase, can be observed. This is similar to the experimentally observed increase of strength in monotonic tests of increasing strain rate. But then it can be concluded that in this latter type of tests,

the "apparent" strength of the material is caused by viscous flow retardation. The faster the strain rate, the higher the retardation and hence the higher the apparent strength.

The limiting case of a monotonic test performed at infinitely high loading rate is of particular interest. In this situation, the stress increment is applied so fast that no viscous flow can take place. Such a test would exhibit elastic stiffness characteristics throughout the range of loading response and it represents a limiting case beyond which no test can be performed. The strength exhibited in this test represents the "true ultimate strength" σ_u of the material. No viscous flow is necessary for fracture. Of course, under laboratory conditions, this ultimate value can never be attained.

In actual engineering tests and, therefore, for realistic loading rates, the development of viscous flow appears to have a detrimental effect on ultimate strength. It can thus be postulated that the "apparent" strength of the material is related to the "true ultimate" strength by means of a decaying function of viscous terms. For a uniaxial test this functional dependency may be expressed, for example, as :

$$\sigma' = \sigma_u - \lambda \cdot \bar{\varepsilon}_{vp} \qquad (2)$$

in which σ' is the experimentally observed strength of the material i.e. the "apparent" strength, λ is a material constant which depends on temperature and $\bar{\varepsilon}_{vp}$ is some measure of viscous flow. The experimental determination of the actual format of Eq. 2 will be presented in a latter section.

In analogy to the uniaxial case, an "ultimate strength surface" can be postulated to define the locus of all states of stress corresponding to the "true ultimate" multiaxial strength of the material $f_u(\underline{\sigma}, \kappa_S) = 0$. κ_S defines the size of the surface and may be a function of viscoplastic straining, viscoplastic work, some other physical measure like temperature or combinations thereof.

As a result of viscous flow, the size of the surface progressively diminishes until it encompasses the imposed state of stress, Fig. 2. This implies that κ_S can be defined as a decaying function of viscous flow. In the proposed model, κ_S has been defined as a function of the maximum tensile viscoplastic strain, i.e. $\kappa_S = \kappa_S(\varepsilon_{vp,t})$. In this study the term "apparent strength surface" will be utilised to characterise any of the ensuing multitude of surfaces. The experimental determination of the response degradation characteristics of the ultimate strength surface will be presented in a latter section.

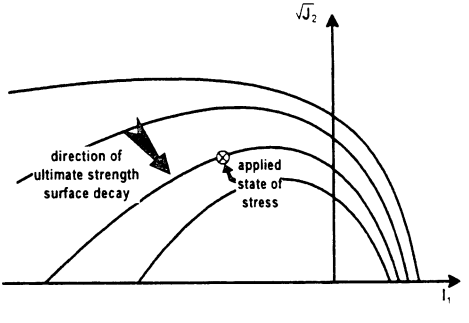

Fig. 2 Ultimate strength surface decay

In a monotonic test, once the apparent strength limit has been exceeded, response degradation follows. Depending on the test conditions it manifests itself by a reduction of material load carrying capacity and the rapid increase of deformations. In a creep test, after a certain amount of viscous flow, initiation of the tertiary creep phase is signaled by the rapid increase of deformations and the eventual loss of load carrying capacity. Because of the fundamental similarity between a creep test and a monotonic test that was pointed out earlier, material strength degradation can also be considered as the cause of the initiation of tertiary creep flow. In the schematic of Fig. 2, initiation of tertiary creep occurs as soon as the imposed state of stress in the material exceeds the progressively diminishing size of the apparent strength surface.

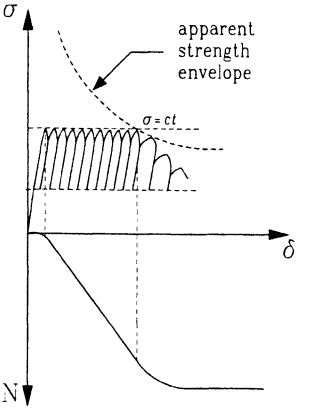

Fig. 3 Cyclic response degradation due to apparent strength decay

Initiation of response degradation typically observed in cyclic tests after several cycles of stress application can also be postulated to occur as a result of the progressively diminishing size of the apparent strength surface. As shown in Fig. 3, as soon as the apparent strength becomes less than the applied stress level, rapid loss of stress carrying capacity is exhibited.

By establishing the fundamental similarities between incremental creep tests and monotonic ones, a unifying constitutive model has been presented capable of simulating the initiation of the response degradation phase of material response. In the following section, the constitutive model will be extended into this range of response.

4 Concepts of material response degradation

Response degradation occurs in a material when the magnitude of the applied stress exceeds the apparent strength. In this section, on the basis of the available experimental evidence, a unifying measure of damage will be proposed for the description of multiaxial response degradation.

In a monotonic uniaxial tension test, initiation of response degradation is accompanied by the development of a fracture zone of small thickness somewhere along the length of the specimen. In a displacement controlled test, as the imposed displacement is increased, progressive damage within the fracture zone causes a degradation in the observed response. Damage does not spread along the length of the specimen. Instead it tends to concentrate within the fracture zone. This phenomenon has been termed in the literature "damage localization". It is only after full annihilation of stress that a discrete discontinuity in the form of a no traction transmitting crack occurs in the material. In this sense two phases of crack response can be identified :

(i) "micro-cracking" phase, during which energy is expended for the creation of a stress free crack surface and,

(ii) "macro-cracking" phase, after the creation of a no traction transmitting crack. "Crack propagation" is then the physical manifestation of the transition from the micro to the macro-cracking phases that neighbouring material points undergo.

Tensile fracture zone initiation, localization and propagation is not a characteristic of uniaxial tension specimens only. By now it is a well established experimental fact that, with the exception of highly confined states of compressive loading, in all other loading ranges, response degradation in aggregate materials is caused predominantly by the nucleation, localization and eventual propagation of splitting cracks, Fig. 4, along planes perpendicular to the maximum principal tensile strain, Nemat-Nasser (4), Willam et al. (5), Vonk (6).

On the basis of this observation, in the proposed constitutive model, after initiation of response degradation, starting from the direction of the maximum principal tensile strain, a system of three mutually orthogonal axes is set up along the directions of the three principal strains. In all subsequent steps of the analysis, the stiffness characteristics of the material along any of these axes degrade whenever the corresponding strain exceeds the strain at initiation of response degradation.

4.1 Numerical simulation of response degradation

As soon as the above mentioned criterion of response degradation initiation is fulfilled along a principal strain axis, a cracking plane is postulated to develope in the original volume of the material in a direction perpendicular to this axis. In subsequent steps, opening of the crack introduces an additional strain component so that the total strain vector can be written as:

$$^{t+\Delta t}\underline{\varepsilon} = {}^{t+\Delta t}\underline{\varepsilon}_{e} + {}^{t+\Delta t}\underline{\varepsilon}_{vp} + \underline{\dot{N}} \cdot {}^{t+\Delta t}\underline{\varepsilon}_{cr,l} \qquad (3)$$

in which $\underline{N}$ is the strain transformation matrix from the crack plane to the global axes system, Fig. 5, and $\underline{\varepsilon}_{cr,l}$ is the vector of crack strains on the crack plane.

At the time step $t + \Delta t$, $\underline{\varepsilon}_{vp}$ can be estimated by means of a forward Euler scheme as :

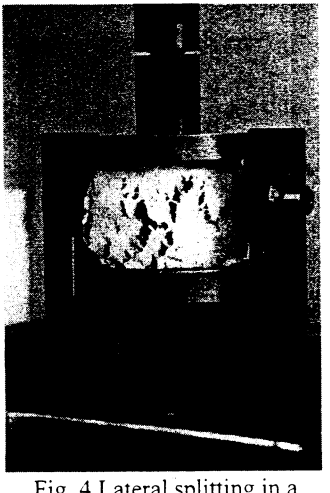

Fig. 4 Lateral splitting in a uniaxial compression test on asphalt specimen

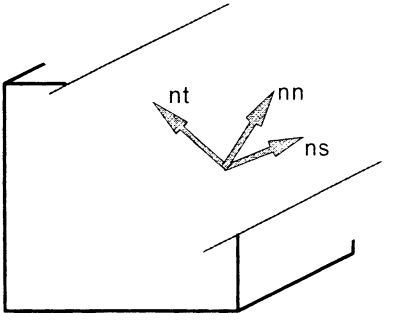

Fig. 5 Crack plane axes system

$$^{t+\Delta t}\underline{\varepsilon}_{vp} = {}^{t}\underline{\varepsilon}_{vp} + {}^{t}\dot{\underline{\varepsilon}}_{vp} \cdot \Delta t \tag{4}$$

Also, on the crack plane :

$$^{t+\Delta t}\underline{\sigma}_{cr,l} = {}^{t+\Delta t}\underline{D}_{cr,l} \cdot {}^{t+\Delta t}\underline{\varepsilon}_{cr,l} \tag{5a}$$

in which :

$$\underline{D}_{cr,l} = \begin{bmatrix} D_{nn} & D_{ns} & D_{nt} \\ D_{sn} & D_{ss} & D_{st} \\ D_{tn} & D_{ts} & D_{tt} \end{bmatrix} \tag{5b}$$

is the secant stiffness of the crack. The off-diagonal terms enable interaction between the normal and the tangential stress components. In case of macro-cracks, the numerical values of these terms can be physically related to the phenomenon of aggregate interlock and their values can be determined experimentally, Walraven (7). In the case of micro-cracks, for which the proposed model is intended, there is by now a consensus of opinion that at this phase of response micro-cracking develops in Mode I fashion, van Mier et al. (8). As a result, the actual values of the off-diagonal coefficients are of no great importance and can be specified as zero, Rots et al. (9).

In the direction perpendicular to the crack plane, the variation of D_{nn} during the time interval dt can be expressed by means of an Euler integration scheme as :

$$^{t+\Delta t}D_{nn} = {}^{t}D_{nn} + {}^{t}\left(\frac{\partial D_{nn}}{\partial t}\right) \cdot dt \tag{6a}$$

In the proposed model, stiffness degradation is considered as the physical manifestation of the development of damage in the material. As mentioned earlier, the latter is postulated to depend on the magnitude of cracking strain $\varepsilon_{cr,\,nn}$. For this reason the rate of damage can be expressed as :

$$\begin{aligned} {}^{t}\left(\frac{\partial D_{nn}}{\partial t}\right) &= {}^{t}\left(\frac{\partial D_{nn}}{\partial \varepsilon_{cr,\,nn}}\right) \cdot {}^{t}\left(\frac{\partial \varepsilon_{cr,\,nn}}{\partial t}\right) \\ &= {}^{t}\left(\frac{\partial D_{nn}}{\partial \varepsilon_{cr,\,nn}}\right) \cdot {}^{t}\dot{\varepsilon}_{cr,\,nn} \end{aligned} \tag{6b}$$

By means of a strain based formulation $\dot{\varepsilon}_{cr,\,nn}$ can be related to the cracking strain $\varepsilon_{cr,\,nn}$ via a functional relationship of the form :

$$\dot{\varepsilon}_{cr,\,nn} = f\left(\varepsilon_{cr,\,nn}\right) \tag{7}$$

The procedure for the experimental determination of the parameters of Eq. 6(b) will be presented in the next section.

In the transverse crack directions, the original G modulus of the material is postulated to degrade due to crack opening as :

$$^{t+\Delta t}D_{tt} = \left(1 - \frac{\varepsilon_{cr,\,nn}}{\varepsilon_{cr,\,nn_{\max}}}\right) \cdot G \tag{8}$$

5 Experimental determination of model parameters

Ideally, results from true triaxial tests at different stress paths, rates and temperatures are required if the full simulation capabilities of the model are to be relished. Nevertheless, in the absence of such results, a methodology has been developed which enables determination of the model parameters on the basis of simple uniaxial tests. Two types of tests are necessary : (a) monotonic compression and tension tests and, (b) incremental creep tests. In this contribution the methodology pertaining to the determination of the response degradation parameters of the model will be presented. Tests were conducted on an asphalt concrete mix of type 0/16 with 6% bitumen 80/100.

5.1 Monotonic uniaxial tensile tests

Tensile tests at different loading rates and temperatures have been performed. Typical results are shown in Fig. 6. A relationship has been developed for the apparent asphalt tensile strength as a function of temperature T and loading rate $\dot{\delta}$:

$$\sigma'_t = \begin{cases} e^{1.3} & \text{for} \quad T \le 10\ ^oC \\ e^{1.3} - \dfrac{5 * 10^{-5} \cdot T^{3.3}}{1.75 + \dot{\delta}} & \text{for} \quad T > 10\ ^oC \end{cases} \tag{9}$$

The ultimate tensile strength can be evaluated from Eq. 9 by considering the limit as $\dot{\delta} \longrightarrow \infty$.

As postulated earlier, for a given temperature, the degradation of the apparent strength values can be related to the amount of accumulated viscoplastic strain.

A formalistic relation expressing the influence of both, accumulated viscoplastic strain and temperature on the apparent tensile strength has been derived:

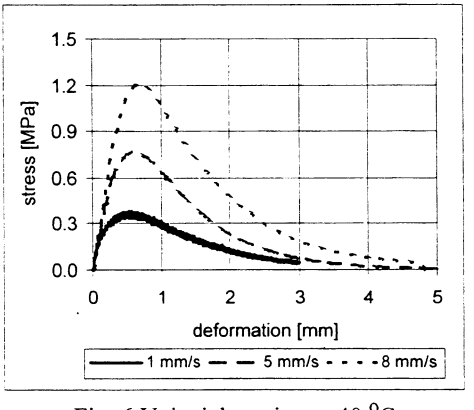

Fig. 6 Uniaxial tension at 40 °C

$$\sigma'_t = \sigma_{tu} - \lambda \cdot \varepsilon_{vp} \tag{10a}$$

in which λ is a material constant which depends on temperature T :

$$\lambda = \begin{cases} 0 & \text{for} \quad T \le 10\ ^oC \\ 25 \cdot T - 100 & \text{for} \quad T > 10\ ^oC \end{cases} \tag{10b}$$

On the basis of the monotonic tensile tests, the relationship between σ and crack openenig w was determined as:

$$\sigma = \sigma'_t \left(1 - \frac{w}{w_{max}}\right) e^{-\alpha \cdot w} \tag{11}$$

in which α is a material parameter that describes the rate of decay and w_{max} is the maximum crack at complete tensile strength annihilation.

For finite element computations, the crack opening w is smeared over a certain width within the finite element which, has become known in the literature as the characteristic length l_c. Following Rots et al. (9), the resulting smeared crack strain ε_{cr} is defined from :

$$w = l_c \cdot \varepsilon_{cr} \tag{12}$$

By means of Eqs. 11 and 12, the secant modulus D_{nn} can be determined. Then the term $\left(\partial D_{nn} / \partial \varepsilon_{cr,\,nn} \right)$ of Eq. 6b can be computed.

5.2 Incremental creep test

For the purpose of determining the relation between the hardening characteristics of the viscous flow surface and the measured visco-plastic strain, incremental creep tests were carried out. A typical curve is shown in Fig. 7. Initiation of tertiary creep is indicated by the rapid increase of the deformation rate after day 16, leading eventually to material destruction. During the tertiary phase of a tensile creep test, the total strain rate is postulated to consist of two parts :

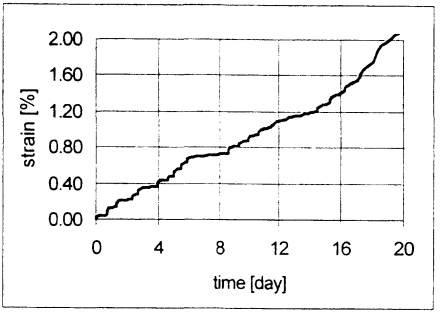

Fig. 7 Incremental creep test

$$\dot{\varepsilon}_{tertiary} = \dot{\varepsilon}_{vp} + \dot{\varepsilon}_{cr} \tag{13}$$

In Eq. 13, $\dot{\varepsilon}_{vp}$ is a constant strain rate equal to that of the secondary creep flow and $\dot{\varepsilon}_{cr}$ is an additional strain rate due to the progressive development of damage in the material. At any time t after initiation of the tertiary phase, the observed strain is :

$$\varepsilon = \varepsilon_{II} + \dot{\varepsilon}_{vp} \cdot t + \varepsilon_{cr} \tag{14}$$

in which ε_{II} is the strain at initiation of the tertiary phase. From the above two equations the form of Eq. 7 can be determined.

6 Study of the dynamic nonlinear response of a road pavement

In this section, computational results from the application of the proposed material model to the study of the dynamic non-linear response of a pavement structure consisting of various layers of viscous materials will be presented. The particular case of pavement excitation by means of a Falling Weight Deflectometer (FWD) test is considered. The FWD essentially consists of a large mass, that is dropped from a certain height onto a set of buffers mounted to a circular foot plate. The resulting shock pulse closely approximates a half sine wave. The peak of this shock pulse is of the same magnitude as would be recorded at the pavement surface under a truck load. Deflection sensors are used to record the vertical displacements at the

surface of the pavement. These deflection data are commonly used to estimate layer moduli and to infer critical strains for rehabilitation purposes.

CAPA-3D was utilized for the simulation of a pavement consisting of a top layer of asphalt concrete 150 mm thick, a granular sub-base layer 250 mm thick and a sand subgrade extending to a depth of 15 m. Because of symmetry, a quarter of the pavement has been simulated. The properties of the aspahlt concrete mix have been determined, for a temperature of T~20 °C, Table 1. Parameters γ, β, m, n, R, and α_0 control the viscous response of the constituent materials, Scarpas et al. (3) and Γ is the viscosity.

Material	γ	β	m	n	R	α_0	Γ
Asphalt concrete	0.087	0.	-0.5	2.	0.16	0.0865	1.5E-09
Granular subbase	0.087	0.	-0.5	2.5	0.	0.05	0.
Sand subgrade	0.087	0.	-0.5	2.5	0.	0.05	0.

Table 1. Material parameters

The pavement was subjected to a sinusoidal pulse of 25 ms duration and 0.707 MPa stress amplitude. The radius of the loaded area was 150 mm.

Time snapshots of the first 40 ms of the pavement surface deflections are shown in Fig. 8. Propagation of the wave-front from the center of the load towards the edges of the pavement can be noticed. Due to the non-linear nature of the asphaltic material, the deformations tend to localize in a narrow band around the load.

Time snapshots of the horizontal and vertical displacement components of a material point at the surface of the pavement, 18 mm from the load centre line are shown in Fig. 9. The arrows indicate the direction of motion in time. The elliptical motion indicates the dominance of the Rayleigh wave components at the surface.

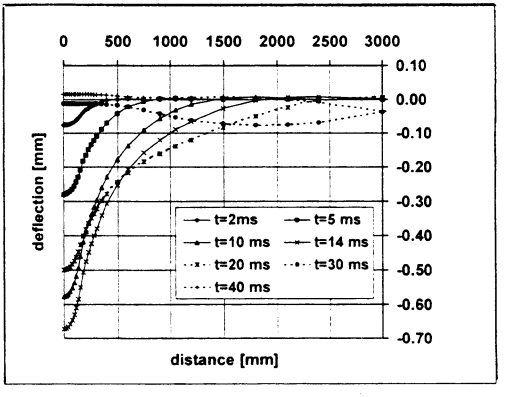

Fig. 8 In-time response of pavement surface

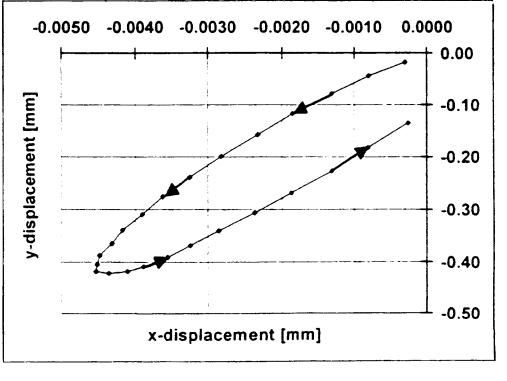

Fig. 9 Surface Rayleigh wave components

Parametric studies are currently carried out in order to investigate the interaction between pulse and pavement characteristics. By means of the analyses valuable insight can be gained for development of adequate FWD calibration procedures.

7 Conclusions

In this contribution a material constitutive model was presented capable of simulating the response degradation characteristics of viscoplastic-fracturing materials. In parallel with the development of the model, an experimental investigation was carried out on an asphalt concrete mix for the purpose of model calibration. Explicit methodologies have been derived and presented for the determination of the relevant model controlling parameters. Implementation of the constitutive model in the finite element system CAPA-3D has enabled the study of various aspects of the dynamic non-linear response of a range of engineering structures. Once the mechanisms leading to a particular phenomenon are understood, design oriented phenomenological models can be derived for use in engineering practise.

References

1. Perzyna P. Fundamental problems in viscoplasticity, *Advances in Applied Mechanics*, 1966, **9**, 243-377.
2. Scarpas A. *CAPA-3D Finite elements system - User's Manual, Parts I, II and III*, Faculty of Civil Engineering, TU-Delft, 1992.
3. Scarpas, A., Al-Khoury, R.I.N., van Gurp, C.A.P.M. and Erkens, S.M.J.G. Finite Elements Simulation of Damage Development in Asphalt Concrete Pavements, 8-th International Conference on Asphalt Pavements, Seattle, 1997, accepted for publication.
4. Nemat-Nasser S. and Horii H. Compression-induced nonplanar crack extension with application to splitting, exfoliation and rockburst, *Journal of Geophysical Research*, 1982, **87**, 6805-6821.
5. Willam K., Hurlbut B. and Sture S. Experimental and constitutive aspects of concrete failure, in FE Analysis of RC Structures, pp. 226-254, *Proceedings of the US-Japan Seminar on FE Analysis of RC Structures*, Tokyo, Japan, 1986, ASCE Special Publication, 1986.
6. Vonk, R.A. A micromechanical investigation of softening of concrete loaded in compression, *Heron*, 1993, **38**, No. 3.
7. Walraven, J.C. *Aggregate interlock: A theoretical and experimental analysis*, Ph.D. Thesis, Faculty of Civil Engineering, TU-Delft, Delft University Press, 1980.
8. van Mier, J.G.M. and Nooru-Mohamed, M.B. Fracture of concrete under tensile and shear-like loadings, in Fracture Toughness and Fracture Energy, (ed H. Mihashi, H. Takahashi & F. Wittmann), pp. 549-563, *Proceedings of the International Workshop on Fracture Toughness and Fracture Energy*, Sendai, 1988, A.A. Balkema, Rotterdam, 1989.
9. Rots J.G., Nauta P., Kusters G.M. and Blaauwendraad J. Smeared crack approach and fracture localization in concrete, *Heron*, 1985, **30**, No. 1.